molecules

MDPI

Article

Tautomerism in Azo and Azomethyne Dyes: When and If Theory Meets Experiment

Liudmil Antonov

Institute of Organic Chemistry with Centre of Phytochemistry, Bulgarian Academy of Sciences, Sofia 1113, Bulgaria; lantonov@orgchm.bas.bg

Received: 3 June 2019; Accepted: 14 June 2019; Published: 17 June 2019

Abstract: The performance of 26 hybrid density functionals was tested against a tautomeric dataset (TautData), containing experimental information for the keto-enol tautomeric equilibrium in 16 tautomeric azodyes and Schiff bases in cyclohexane, carbon tetrachloride and acetonitrile. The results have shown that MN12-SX, BHandH and M06-2X can be used to describe the tautomeric state of the core structures in the frame of ~0.5 kcal/mol error and correctly predict the tautomeric state in respect of dominating tautomeric form. Among them MN12-SX is the best performer, although it fails to describe the nonplanarity of some of the enol tautomers. The same experimental dataset was used to develop and test a special DFT functional (TautLYP) aimed at describing the tautomeric state in azo- and azomethyne compounds in solution when nonspecific solvents are used.

Keywords: DFT; tautomerism; azonaphthols; Schiff bases; optical spectroscopy; chemometrics

1. Introduction

Prototropic tautomerism [1–12] is one of the most important phenomena in organic chemistry despite the relatively small proportion of molecules in which it can occur. Tautomers are the chameleons of chemistry, capable of changing by a simple change of environment from an apparently established structure to another, then back again when the original conditions are restored. The importance of the tautomerism and proton transfer [12] in the life science, drug design and technology makes it vital to know and/or to predict which tautomer is the major one, since not only the structure, but chemical properties are bound up with this.

According to the classification of dyes, more than half of them are azo compounds and a substantial part are tautomeric or potentially tautomeric [13–16]. Compound **1** (Scheme 1), one of the first tautomeric compounds discovered [17] and studied almost one and half century [18], is a typical example. Experimental and theoretical investigations of the tautomerism have a solid practical reason, because the color and the stability of the azodyes are strongly influenced by their tautomerism [19]. The Schiff bases are another important class of dyes exhibiting interesting photo- and thermochromic properties and bioactivity, again, in most of the cases, related to their tautomerism [20–22].

While the potentially tautomeric structures can be easily distinguished either theoretically or experimentally [23], the study of real tautomeric equilibria in solution is a challenge. On one side, the real equilibrium from the viewpoint of the detection limits of analytical chemistry means Gibb's free energy in the range roughly from −2 to +2 kcal/mol, which is a challenge for quantum chemistry even now [24]. On the other side, the exact estimation of the ΔG values (derived from the tautomeric constant K_T, defined as keto/enol, [**K**]/[**E**] ratio, Scheme 2), requires isolated tautomeric forms, a condition that is impossible in most of the cases. A major breakthrough in the UV-Vis spectroscopy was the development of chemometric methods to obtain the absorption spectra of the individual tautomers, even though these are never present in their pure form, and then to estimate the tautomeric constants as function of a number of external parameters (temperature, irradiation, solvents, pH, and concentration) [25,26].

The availability of such experimental data has given us the opportunity to check the reliability of the quantum-chemical methods in predicting the position of the tautomeric equilibria in selected azonaphthols and related Schiff bases in solution [24,27]. The results for these dyes and for the tautomeric compounds in general, clearly indicate that there is no universal reliable theoretical solution and the predicted tautomeric shift, often wrong, depends strongly on the theoretical background.

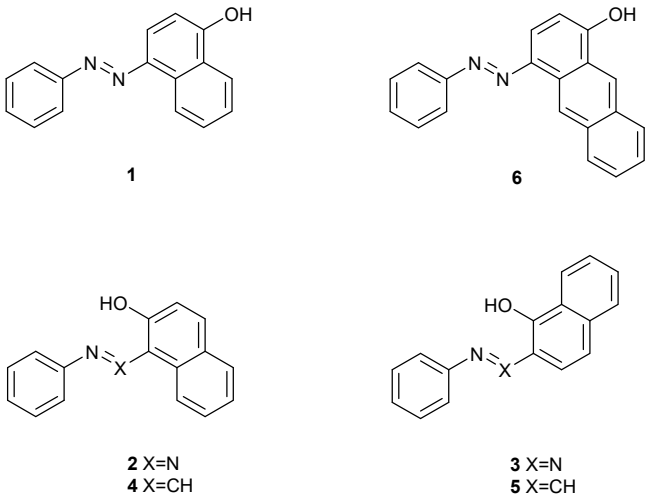

Scheme 1. Core tautomeric dyes used in this study.

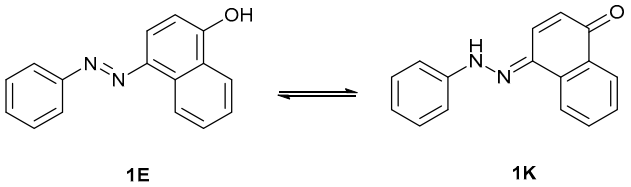

Scheme 2. Tautomeric equilibrium in **1** given as an example for the structures from Scheme 1.

The affordable accuracy of quantum chemistry in respect of correct prediction of tautomeric equilibria depends on one side on the molecular size and particularly on the total number of atoms, and on the other, on the requirement to take into account the effect of the solvent. Currently molecules with up to 10 atoms can be very accurately studied by coupled cluster theory, similar to 100 atoms with second order Moller-Plesset perturbation theory (MP2), similar to 1000 atoms with DFT and beyond this number with semiempirical quantum chemistry and force-field methods [28]. The previous results obtained by using MP2 for tautomeric azonaphthols have shown that this level of theory very strongly overestimates the enol tautomer irrespective of the used basis set [27]. This along with the computational affordability directs the possible solution into the DFT field. There is a substantial number of datasets used for benchmarking and/or density functional development in the field of thermochemistry, kinetics, and noncovalent interactions [29–33]. To our best knowledge, no attempts have been made to develop a density functional that describes reasonably well the relative energies of substantial set of tautomeric compounds. The obvious reason is that there is no way for systematic improvement of the DFT functionals performance, especially in the absence of experimental data to test the theoretical development.

Therefore, the aim of the current communication is to introduce a tautomeric dataset (TautData), containing reliable and precise experimental data for the tautomeric equilibrium of basic dye structures in solution (Schemes 1 and 3) and to test how the most promising density functionals, MP2 and coupled cluster methods predict the tautomerism of these compounds. In addition, the available experimental information has been used to develop a cheap solution for correct description of the tautomerism of the dyes listed in Scheme 1. The reliability of the new tautomeric functional (TautLYP) is compared with the others in a large collection of dyes derived from the structures in Scheme 1 (Scheme 3).

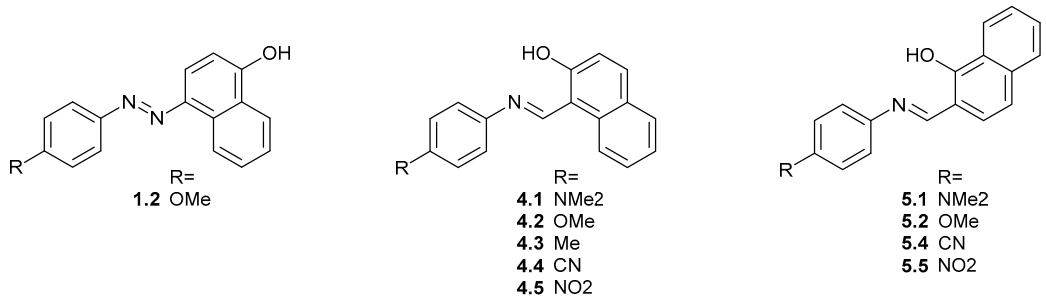

Scheme 3. Substituted compounds derived from **1**, **4** and **5**.

2. Results and Discussion

The compounds used for benchmarking and DFT functional development (Scheme 1) represent core structures for azo- and corresponding azomethyne dyes [15,34]. Compound **1** is one of the first tautomeric dyes discovered. Compounds **2** and **3** are the core structures of the major class (>60%) of the industrial azodyes (neutral and their metal complexes). Compounds **4** and **5** exhibit interesting photochemical and thermochemical properties in solution and solid state [20,35]. Their tautomeric behavior in solution is very different. In **2**–**5** the existing intramolecular hydrogen bonding limits the effect of the solvent on the shift of the tautomeric equilibrium. As a result, the tautomeric constants can be changed by change of the solvent in a relatively narrow range. The specific effect of the solvent is also different; the strength of the intramolecular hydrogen bonding in **4** and **5** limits the effect of the proton acceptor solvents, while the same bond in **2** and **3** is weak and can be easily broken [36,37]. The proton acceptor/donor sites in the tautomers of **1** are accessible for the solvents, which allows for a large scale of the tautomeric constant change [38]. In **6,** due to aromatic reasons, the tautomeric equilibrium is shifted almost fully to the keto form [13,39,40]. The structural effects are also different; substitution on para position of the phenyl ring in the azodyes leads to a shift of the tautomeric equilibrium towards the enol form when electron donor group is implemented and vice versa. The effect of the substitution in the Schiff bases is limited due to the substantial nonplanarity of the phenyl ring in respect of the overall conjugated system [41].

Keeping in mind that as a rule the solvent effect on the tautomeric equilibrium is specific, experimental data obtained in cyclohexane are used for the benchmarking in the current study. In this way it is assumed that the implicit solvation describes the effect of the solvent. The corresponding ΔG values at room temperature for compounds **1**–**6** are listed in the last row of Table 1. The positive values indicate a more stable enol form and vice versa. It is clearly seen that the set of **1**–**6** covers the whole range of changes, from 1.42 in **4** to −1.31 in **6**, which along with the variety of structural features discussed above, makes the selection of dyes very suitable for benchmarking. The experimental data are compared in Table 1 to the predicted relative stabilities of the tautomers generated by variety of hybrid GGA and meta-GGA density functionals. Their order of appearance depends on the statistical data of their performance presented in Table 2. The selection of the functionals is related to their popularity, use in investigation of tautomeric systems and previous benchmarking of **1** [18] and **1**–**3** [27].

Table 1. Experimental ($\Delta G_{experimental}$) and predicted relative stabilities ($\Delta E_{predicted}$) * of the tautomers of **1–6** in cyclohexane **.

Functional Name	$\Delta E_{predicted}$ kcal/mol						Linearity: $\Delta E_{predicted} = a.\ \Delta G_{experimental} + b$		
	1	**2**	**3**	**4**	**5**	**6**	***a***	***b***	**R *****
TautLYP	1.49	0.39	0.22	1.54	0.80	−1.35	1.04	−0.01	0.996
MN12-SX [42]	2.00	0.48	−0.35	1.58	0.79	−0.60	0.91	0.25	0.936
BHandH [43]	1.01	0.22	−0.42	1.50	0.68	−2.15	1.22	−0.39	0.988
M06-2X [44]	1.88	0.82	0.18	2.23	1.41	−1.19	1.19	0.38	0.996
HF [30,45]	*1.16*	*0.28*	*−0.22*	*0.55*	*−0.14*	*−2.83*	*1.19*	*−0.71*	*0.906*
SOGGA11-X [46]	0.73	−0.65	−1.40	0.42	−0.42	−2.25	1.03	−1.04	0.975
M11 [47]	0.83	−0.89	−1.34	0.51	−0.13	−2.59	1.19	−1.11	0.986
BHandHLYP [43]	0.42	−0.65	−1.30	0.53	−0.25	−2.80	1.17	−1.18	0.996
CAM-B3LYP [48]	−0.44	−1.15	−1.71	0.31	−0.41	−3.58	1.27	−1.71	0.978
HISSbPBE [49]	−0.70	−1.03	−1.83	0.31	−0.64	−3.60	1.23	−1.78	0.965
ωB97X [50]	−0.15	−1.39	−1.88	0.07	−0.62	−3.59	1.28	−1.81	0.995
PBE0 [51]	−0.90	−1.08	−1.90	0.37	−0.54	−3.57	1.21	−1.79	0.951
PBEh1PBE [52]	−0.92	−1.19	−2.01	0.25	−0.65	−3.59	1.20	−1.87	0.958
APF [53]	−1.07	−1.19	−2.01	0.27	−0.63	−3.71	1.22	−1.91	0.944
ωB97X-D [54]	−0.60	−1.41	−2.00	0.08	−0.66	−3.81	1.29	−1.96	0.984
HSE06 [55]	−1.04	−1.20	−2.05	0.20	−0.72	−3.63	1.18	−1.92	0.951
LC-ωPBE [56]	−0.87	−1.41	−1.86	0.35	−0.34	−4.46	1.51	−2.08	0.950
APFD [53]	−1.45	−1.29	−2.11	0.26	−0.62	−4.07	1.28	−2.10	0.914
B3PW91 [57,58]	−1.34	−1.33	−2.17	0.14	−0.77	−3.91	1.22	−2.09	0.932
X3LYP [59]	−1.19	−1.49	−2.26	−0.16	−1.00	−3.80	1.14	−2.14	0.963
MP2 [60]	*3.70*	*2.03*	*1.24*	*3.75*	*3.18*	*1.45*	*0.96*	*2.14*	*0.902*

Table 1. *Cont.*

Functional Name	$\Delta E_{predicted}$ kcal/mol						Linearity: $\Delta E_{predicted} = a.\ \Delta G_{experimental} + b$		
	1	**2**	**3**	**4**	**5**	**6**	***a***	***b***	**R *****
B3LYP [61,62]	−1.36	−1.58	−2.37	−0.24	−1.09	−3.93	1.15	−2.26	0.957
TPSSh [63]	−1.61	−1.49	−2.35	−0.31	−1.22	−4.01	1.11	−2.31	0.930
τ-HCTHhyb [64]	−1.87	−1.58	−2.45	−0.12	−1.02	−4.31	1.22	−2.42	0.903
N12SX [42]	−1.95	−1.79	−2.58	−0.22	−1.16	−4.59	1.28	−2.60	0.913
TPSS [65]	−2.44	−1.73	−2.64	−0.68	−1.58	−4.58	1.08	−2.74	0.861
O3LYP [66,67]	−2.44	−2.06	−2.90	−0.48	−1.43	−4.85	1.25	−2.90	0.889
BMK [68]	−3.01	−3.16	−3.94	−0.74	−1.65	−5.99	1.57	−3.76	0.906
M06-HF [44]	6.34	4.92	4.55	4.00	3.81	2.72	0.70	4.09	0.609
experiment ****	***1.35***	***0.42***	***−0.24***	***1.42***	***0.94***	***−1.31***			

* difference between the energies of the keto and enol tautomeric forms, positive value indicates more stable enol tautomer and vice versa; ** see Materials and methods for the computational details and experimental procedures; *** correlation coefficient; **** ΔG values ($\Delta G_{experimental}$), derived from the tautomeric constant in cyclohexane at room temperature, the corresponding molar fractions [in %] of the enol tautomer are 9, 33, 60, 8, 17, 90 for **1**–**6** correspondingly.

Table 2. Statistical parameters of the benchmarking (Table 1).

Functional Name	Type *	HF Exchange [%]	MAE **	MAPE *** [%]	MSE ****	MSPE ***** [%]
TautLYP	GH-GGA	43.79	0.08	8.4	0.01	84.6
MN12-SX	RSH-mGGA	25–0	0.31	31.5	0.16	1326
BHandH	GH-GGA	50	0.32	41.5	0.16	2336
M06-2X	GH-mGGA	54	0.46	71.5	0.25	8019
HF		100	0.64	58.1	0.72	5307
SOGGA11-X	GH-GGA	40.15	1.03	179	1.11	56,652
M11	RSH-mGGA	42.8–100	1.03	182	1.14	57,162
BHandHLYP	GH-GGA	50	1.11	179	1.26	50,795
CAM-B3LYP	RSH-GGA	19–65	1.59	254	2.61	100,203

Table 2. *Cont.*

Functional Name	Type *	HF Exchange [%]	MAE **	MAPE *** [%]	MSE ****	MSPE ***** [%]
HISSbPBE	RSH-GGA	0–60–0	1.68	265	2.97	109,721
ωB97X	RSH-GGA	15.77–100	1.69	278	2.95	124,477
PBE0	GH-GGA	25	1.70	271	3.08	118,265
PBEh1PBE	GH-GGA	25	1.78	287	3.34	133,408
APF	GH-GGA	23	1.82	290	3.53	134,506
ωB97X-D	RSH-GGA + D	22.2–100	1.83	296	3.48	139,486
HSE06	RSH-GGA	25–0	1.84	294	3.54	139,086
LC-ωPBE	RSH-GGA	0–100	1.86	289	3.94	127,711
APFD	GH-GGA + D	23	1.98	310	4.29	152,067
B3PW91	GH-GGA	20	1.99	316	4.23	159,313
X3LYP	GH-GGA	21.8	2.08	333	4.44	176,504
MP2		100	2.13	298	4.72	115,308
B3LYP	GH-GGA	20	2.19	352	4.95	196,692
TPSSh	GH-mGGA	10	2.26	353	5.31	193,046
τ-HCTHhyb	GH-mGGA	15	2.32	365	5.75	210,342
N12SX	RSH-GGA	25–0	2.48	391	6.52	239,972
TPSS	mGGA	0	2.71	411	7.72	253,502
O3LYP	GH-GGA	11.61	2.79	442	8.23	307,829
BMK	mGGA	42	3.51	586	13.1	582,436
M06-HF	GH-mGGA	100	3.96	709	16.5	930,805

* the following abbreviations are used in this column: +D, addition of dispersion corrections; GH, global hybrid; RSH, range-separated hybrid; GGA, generalized gradient approximation; mGGA, meta-GGA.;** Mean Absolute Error; *** Mean Absolute Percentage Error; **** Mean Square Error; ***** Mean Square Percentage Error.

It seems from the data that no one of the existing density functionals fits the experiment perfectly. Linearity, shown in Table 1, can be used for monitoring whether the general tendency of predicting is correct or not. Basically, the perfect situation should have correlation and slope tending to 1 and a zero intercept. Some of the functionals give highly correlated results (M06-2X, BHandHLYP, ωB97X), while in other cases the predictions scatter (M06-HF, TPSS, O3LYP). The description the tautomeric state of the studied compounds is quite unrealistic in the case of HF and MP2. In most of the cases the slope tends to 1, which with the relatively good correlations indicates that corresponding functional correctly describes the relative structural aspects of the tautomerism (SOGGA11-X for instance). The intercept roughly shows if the theory overestimates one or another tautomer in the tautomeric mixture; most of the functionals overestimate the stability (negative slope) of the keto tautomer, some of them very strongly (CAM-B3LYP and below). The statistical data in Table 2 follows the major conclusions up to now. Generally it is very difficult to write a clear conclusion about tendencies; the best behaving density functionals belong to different classes (GH/RSH mGGA/GGA), so there is no clear relation with the HF exchange and even functionals belonging to the same family (BHandH, BHandHLYP, B3LYP) behave in a different way. It is obviously that MN12-SX, BHandH and M06-2X can be used to describe the tautomeric state of **1**–**6** in the frame of ~0.5 kcal/mol error and correctly predict the tautomeric state in respect of dominating tautomeric form (i.e. positive/negative ΔE). In the frame of 1 kcal/mol precision SOGGA11-X, M-11 and BHandHLYP could be also used. However, this is a general statistical conclusion which should be taken with care. If BHandHLYP is considered one example, it predicts molar fraction of the keto tautomer as 33, 75, 90, 29, 61, 99 (in %, calculated from the corresponding ΔE values in Table 1) for **1**–**6** respectively. At the same time the experimental values are 9, 33, 60, 8, 17, 90, which means that the position of the tautomeric equilibrium in **2** and **5** is predicted completely wrong, while the values of **1**, **3** and **4** strongly underestimate the contribution of the enol tautomer.

It is obvious from Tables 1 and 2 that TautLYP describes the experimental dataset much better compared to the next best performers, which is not surprising since it is fitted against exactly this experiment. Therefore, it is needed to check it and the others' reliability against different datasets. For this purpose, structural data (bond length and dihedral angles) of **1** and **6** will be used along with equilibrium data for the dyes from Scheme 3.

Currently, structural data for the enol and keto tautomers of **1** are available in the literature [18] along with data for the fixed enol tautomer (OMe compound) of **6** [69]. In the case of compounds **2**–**5** even if crystallographic data are available the structures contain contribution of both tautomers [70,71], which makes the structural information unsuitable for benchmarking.

The structural data along with the predicted results for the density functionals from TautLYP to BHandHLYP are collected in Table S1, Supplementary information. In Table 3 the statistical evaluation of the performance of the functionals is given.

The results indicate that all studied DFT functionals describe the bond lengths reasonably well. The differences are very slight (except in the case of BHandH) to speculate about best performers. In respect of the angles description two distinguished groups are seen, depending on the non-planarity description. MN12-SX, BHandH and M11 predict the enol form planar, which reflects in substantially higher MAE and MAPE. In respect of the total MAPE TautLYP and M06-2X are the best performers.

Experimental data in CCl_4 and acetonitrile for the tautomeric state of the core structures and their substituted compounds are collected in Table 4. As in the case of cyclohexane, the solvents have been selected to avoid specific solute-solvent interactions and to assume implicit solvation model. The performance of the best functionals from Table 2 is compared with that of B3LYP in Table 5. The statistical results are based on the data from Table S2. It is seen that TautLYP predicts the experiment slightly better comparing to MN12-SX, but the information from Table 3 should also be taken into account for the final decision which of them to use. Comparing to B3LYP both have MAPE in orders better.

Table 3. MAE and MAPE of the structural elements description of the tautomers of **1** and **6**.

Functional Name	MAPE [%]			MAE		Non-Planarity Description *
	Bonds	Angles	Total	Bonds [Å]	Angles [°]	
TautLYP	3.31	42.27	45.57	0.05	3.81	yes
MN12-SX	2.95	199.70	202.65	0.04	20.72	no
BHandH	4.95	199.99	204.93	0.07	20.75	no
M06-2X	2.61	114.56	117.17	0.04	12.26	yes
HF	4.53	48.04	52.57	0.06	4.34	yes
SOGGA11-X	2.76	140.41	143.16	0.04	14.91	no (**1**), yes (**6**)
M11	2.55	200.00	202.55	0.03	20.75	no
BHandHLYP	3.38	141.55	144.93	0.05	15.00	no (**1**), yes (**6**)

* according to the crystallographic data the Ph and naphthalene rings in the enol forms of **1** and **6** are twisted in respect of the N=N group (see Table S1 and Scheme S1 for more information).

Table 4. Experimentally determined ΔG values in kcal/mol units.

Cmpd	R	Solvent	
		CCl_4	CH_3CN
1	H		−0.03
1.2	OCH_3		1.49
2	H	0.34	−0.15
3	H	−0.39	−0.47
4	H	1.40	0.30
4.1	$N(CH_3)_2$	1.33	0.37
4.2	OCH_3	1.34	0.37
4.3	CH_3	1.33	0.23
4.4	CN	1.42	0.55
4.5	NO_2	1.48	0.47
5	H	0.79	−0.34
5.1	$N(CH_3)_2$	1.12	−0.45
5.2	OCH_3	0.98	−0.20
5.4	CN	0.91	−0.10
5.5	NO_2	1.00	−0.15

Table 5. Performance of the studied DFT functionals in respect of the data from Table 4.

Functional	MAE		MAPE [%]		MAPE [%] C_6H_{12}, CCl_4, CH_3CN
	CCl_4	CH_3CN	CCl_4	CH_3CN	
TautLYP	0.16	0.09	14.9	62.3	85.7
MN12-SX	0.18	0.18	15.8	97.3	144
BHandH	0.17	0.14	18.0	182	242
M06-2X	0.72	0.67	74.5	335	481
B3LYP	1.78	2.08	216	1401	1969

Availability of CCSD(T) data in the gas phase makes possible to compare the results with these of TautLYP. Of course, there is a difference in the linear equations of TautLYP in cyclohexane (Table 1) and in the gas phase (Table 6) in respect of the offset. The gas phase equation gives systematic predominance of the enol tautomers, which is reasonable because the higher dipole moment of the keto forms, giving difference in the implicit solvation model in cyclohexane, is not accounted. Keeping in mind that for the CCSD(T) calculations MP2 optimized geometry is used, in Table 6 the results for TautLYP and TautLYP//MP2 are presented. Although the linearity parameters are almost the same there is difference in the prediction of the ΔE values for the azo compounds in the frame of ~0.2 kcal/mol, which is a result from the increased twisting of the phenyl ring in the MP2 optimization geometry. In the case of **4** and **5** where the angles predicted by TautLYP and MP2 are near, the difference in the ΔE values is small. Comparing MP3//MP2 and MP4//MP2 with TautLYP, it is seen that the former strongly overestimates the keto tautomer, while the latter has relatively good prediction ability. The overall impression for CCSD(T) is that the enol form is overestimated, especially in the case of **6**. A comparison of the CCSD(T) and TautLYP//MP2 predicted ΔE values shows that they are almost identical for **1**, strongly different in **6** and well correlated in the case of **2**–**5** (with a difference of 0.9–1.1 kcal/mol in respect of the enol stabilization by CCSD(T)).

Table 6. Comparison between TautLYP and CCSD(T) in gas phase.

	$\Delta E_{predicted}$ kcal/mol						Linearity: $\Delta E_{predicted} = a.\ \Delta G_{experiment} + b$		
	1	**2**	**3**	**4**	**5**	**6**	***a***	***b***	**R**
TautLYP	2.49	0.80	0.09	2.34	1.57	−0.42	1.09	0.67	0.965
MP2	4.41	2.27	1.41	4.43	3.82	2.09	1.04	2.62	0.837
TautLYP *	2.70	0.63	−0.14	2.38	1.62	−0.21	1.10	0.69	0.922
MP3 *	4.03	2.64	2.11	4.56	4.00	1.11	1.24	2.54	0.976
MP4 *	1.67	0.41	−0.49	2.51	1.84	−0.48	1.10	0.44	0.909
CCSD(T) *	2.77	1.53	0.78	3.40	2.78	0.40	1.10	1.47	0.949

* using MP2 geometry.

Further studies of the performance of TautLYP by using the standard databases for DFT development, as well as comparison with CCSD(T) calculations in solution, could shed light on the applicability of this density functional for general purposes and for predicting the equilibrium state of other tautomeric systems in solution. The calculations are in progress and the results will be reported later.

3. Materials and Methods

In total, 35 compounds (**1**–**6** and derived from them) were synthesized, purified and characterized according to the standard procedures [14,15]. For each of them the protocol for determination of the tautomeric constants as described previously was applied [26,72]. The protocol includes UV-Vis spectra measurements followed by a chemometric data processing [72]. To make the data comparable, all spectra were measured at the same instrumental conditions (scan speed, detector output and spectral slit) on Jasco V570 UV-Vis-NIR double beam spectrometer (JASCO International Co. Ltd., Tokyo, Japan) equipped with a thermostatic cell holder (Huber MPC-K6 thermostat with 1 °C precision (Peter Huber Kältemaschinenbau AG, Offenburg, Germany)) in spectral grade solvents (cyclohexane and acetonitrile, both Multisolvent grade from Sharlau (Scharlab, Barselona, Spain)) at 25 °C. The obtained spectra of each compound were processed using resolution of overlapping bands in order to get the molar fractions of the keto and enol tautomers and their spectral characteristics in the corresponding solvent. The chemometric protocol is described in detail, together with examples in [72]. The tautomeric molar fractions allow for calculation of the tautomeric constant K_T (defined as **[K]**/**[E]**) and hence, evaluation of the corresponding ΔG value, which is finally included in TautData.

For the aims of benchmarking, in the TautData dataset are finally included only precise ΔG values in cyclohexane and acetonitrile, obtained based on molar fractions of the enol tautomer in the frame ±5%. The data for CCl_4 are taken from the literature and are obtained previous by us using the same protocol [36,41,73,74]. Keeping in mind that they are obtained at different time, the precision might be lower comparing to these in cyclohexane and acetonitrile due to slightly different experimental conditions.

The quantum chemical calculations in current study were performed by using Gaussian 09 Rev. D.01 program suite [75]. In all cases 6-31++G** basis set was applied. The hybrid density functionals are used as implemented. All structures were optimized without restrictions in gas phase under tight optimization conditions by using ultrafine grid in the computation of the two-electron integrals and their derivatives. The optimized structures were then characterized as true minima by vibrational frequency calculations. The solvent effect was then described by applying the polarizable continuum model (PCM) in its integral equation formalism variant (IEFPCM) [76]. In the case of MP2 normal optimization conditions were used. In the CCSD(T) [77] single point calculations the convergence on the energy was set to 10^{-6}. For the purpose of benchmarking the ΔE values, representing the energy difference $E_K - E_E$ in the corresponding solvent, are used.

The TautLYP was optimized using the general equation for exchange-correlation functional:

$$E_{XC} = a.E_X^{HF} + b.E_X^{Slater} + c.\Delta E_X^{Becke} + d.E_C^{VWN} + e.\Delta E_C^{LYP} \quad (1)$$

where ΔE_X^{Becke} and ΔE_C^{LYP} are the generalized gradient approximations–the Becke's 1988 exchange functional [57] and the correlation functional of Lee, Yang and Parr [62,78], respectively; E_C^{VWN} is the VWN local-density approximation to the correlation functional [79].

Thus, E_{XC} is governed by 5 parameters, which gives it a high extent of flexibility and possibility to be fitted against experimental data. In this case searching global minimum of the target function S_T was performed according to the following equation:

$$S_T = \frac{1}{n_T}\sum_{i=1}^{n_T}\left(\frac{\Delta G_i^{exp} - \Delta E_i^{E_{XC}}}{\Delta G_i^{exp}}\right)^2 \quad (2)$$

where n_T is the number of the tautomeric compounds included in the fitting (six compounds, Scheme 1), ΔG^{exp} are the experimentally determined Gibb's free energies 25 °C in cyclohexane (as described above) and $\Delta E^{E_{XC}}$ are the relative energies (difference between the energies of the keto and enol tautomeric forms of the same compound optimized in gas phase and calculated in cyclohexane as a single point) calculated with the functional defined by equation (1) at particular values of $a - e$.

The optimization in respect to equation (2) was performed by using advanced simplex optimization of these optimization parameters (m, which means $m + 1$ dimensional optimization space and m vertices of the simplex). In this case $m = 5$. The method of Nelder and Mead was applied [80] for the optimization. The process was terminated when the standard deviation σ^2, defined by Equation (3), became less than 1×10^{-9}.

$$\sigma^2 = \frac{\sum_{j=1}^{m+1}\left(S_{T_j} - \overline{S_T}\right)^2}{m+1} \quad (3)$$

where S_{T_j} is the value of the optimization function (2), defined by a set of $a_j - e_j$ parameters; $\overline{S_T}$ is the average value.

At that stage there are no substantial differences between the $a - e$ values in the m vertices, because the simplex is too small.

In total, ten optimization procedures were performed until the end with a differing orientation of the initial simplex, yielding finally TautLYP with $a = 0.4379$; $b = 0.5178$; $c = 0$; $d = 0.0910$; $e = 0.9174$.

The TautLYP density functional can be used by the following Gaussian 09 input:

BLYP IOp (3/76 = 1000004379,3/77 = 0000005178,3/78 = 0917400910).

4. Conclusions

TautData dataset containing precise information for the position of the tautomeric equilibrium of azodyes and Schiff bases was created. It contains information for 6 compounds in cyclohexane, 13–in carbon tetrachloride and 15–acetonitrile and can be used for benchmarking of density functional development.

Using the information for the position of the tautomeric equilibrium in cyclohexane of 6 core structures of industrially important azo- and azomethyne dyes, a new hybrid density functional, namely TautLYP, was fitted. Its reliability was checked by using the data from TautData, showing very good performance.

Benchmarking of existing DFT functionals was performed by using TautData and available structural information for some of the tautomers. The results have shown that MN12-SX, BHandH and M06-2X can be used to describe the tautomeric state of the core structures in the frame of ~0.5 kcal/mol error and correctly predict the tautomeric state in respect to a dominating tautomeric form. Among them, MN12-SX is the best performer, although it fails to describe the nonplanarity of some of the enol tautomers.

Supplementary Materials: The following are available online at http://www.mdpi.com/1420-3049/24/12/2252/s1, Scheme S1: Skeleton of **1** and **6**, Table S1: Experimental and predicted structural parameters of **1E**, **1K** and **6E**, Table S2: Predicted ΔE values in kcal/mol units.

Funding: This research was funded by Bulgarian Science Fund, grant DCOST01/5/2017 for national support of the COST Action CM1405 (Molecules in motion, MOLIM.

Acknowledgments: The financial support from Bulgarian National Science Fund (project DCOST01/5/2017 for national support of the COST Action CM1405 (Molecules in motion, MOLIM)) and the equipment donations from Alexander von Humboldt Foundation and The Swiss National Science Fund (SCOPES program SupraMedChem@Balkans.Net Institutional partnership project IZ74Z0 160515) are gratefully acknowledged.

Conflicts of Interest: The author declare no conflict of interest.

References

1. Taylor, P.J.; van der Zwan, G.; Antonov, L. Tautomerism: Introduction, history, and recent developments in experimental and theoretical methods. In *Tautomerism: Methods and Theories*; Antonov, L., Ed.; Wiley-VCH: Weinheim, Germany, 2013; pp. 1–24. ISBN 978-3-527-65882-4.
2. Baker, J.W. *Tautomerism*; George Routledge and Sons Ltd.: London, UK, 1934.
3. Eistert, B. *Tautomerie und Mesomerie: Gleichgewicht und '"Resonanz"*; Enke: Stuttgart, Germany, 1938.
4. Elguero, J.; Marzin, C.; Katritzky, A.R.; Linda, P. The tautomerism of heterocycles. In *Advances in Heterocyclic Chemistry*; Academic Press: New York, NY, USA, 1976; ISBN 978-0-12-020651-3.
5. Minkin, V.I.; Olekhnovich, L.P.; Zhdanov, I.A. *Molecular Design of Tautomeric Compounds*; Springer: Dordrecht, The Netherlands, 1988; ISBN 978-94-009-1429-2.
6. Elguero, J.; Katritzky, A.R.; Denisko, O.V. Prototropic tautomerism of heterocycles: Heteroaromatic tautomerism—General overview and methodology. In *Advances in Heterocyclic Chemistry*; Elsevier: Amesterdam, The Netherlands, 2000; Volume 76, pp. 1–84. ISBN 978-0-12-020776-3.
7. Minkin, V.I.; Garnovskii, A.D.; Elguero, J.; Katritzky, A.R.; Denisko, O.V. The tautomerism of heterocycles: Five-membered rings with two or more heteroatoms. In *Advances in Heterocyclic Chemistry*; Elsevier: Amesterdam, The Netherlands, 2000; Volume 76, pp. 157–323. ISBN 978-0-12-020776-3.
8. *Hydrogen-Transfer Reactions*, 1st ed.; Hynes, J.T.; Klinman, J.P.; Limbach, H.; Schowen, R.L. (Eds.) Wiley: Hoboken, NJ, USA, 2006; ISBN 978-3-527-30777-7.
9. Stanovnik, B.; Tišler, M.; Katritzky, A.R.; Denisko, O.V. The tautomerism of heterocycles: Substituent tautomerism of six-membered ring heterocycles. In *Advances in Heterocyclic Chemistry*; Elsevier: Amesterdam, The Netherlands, 2006; Volume 91, pp. 1–134. ISBN 978-0-12-020791-6.

10. Martin, Y.C. Let's not forget tautomers. *J. Comput.-Aided Mol. Des.* **2009**, *23*, 693–704. [CrossRef] [PubMed]
11. *Tautomerism: Methods and Theories*; Antonov, L. (Ed.) Wiley-VCH: Weinheim, Germany, 2014; ISBN 978-3-527-33294-6.
12. *Tautomerism: Concepts and Applications in Science and Technology*; Antonov, L. (Ed.) Wiley-VCH: Weinheim, Germany, 2016; ISBN 978-3-527-33995-2.
13. Gordon, P.F.; Gregory, P. Azo dyes. In *Organic Chemistry in Colour*; Springer-Verlag: Berlin, Germany, 1987; pp. 95–162. ISBN 978-3-642-82959-8.
14. Kelemen, J. Azo-hydrazone tautomerism in azo dyes. I. A comparative study of 1-phenylazo-2-naphthol and 1-phenylazo-2-naphthylamine derivatives by electronic spectroscopy. *Dye. Pigment.* **1981**, *2*, 73–91. [CrossRef]
15. Zollinger, H. *Color Chemistry: Syntheses, Properties, and Applications of Organic Dyes and Pigments*, 3rd ed.; Wiley-VCH: Zürich, Switzerland; Weinheim, Germany, 2003; ISBN 978-3-906390-23-9.
16. Christie, R.M. *Colour Chemistry*, 2nd ed.; Royal Society of Chemistry: Cambridge, UK, 2015; ISBN 978-1-84973-328-1.
17. Zincke, T.; Bindewald, H. Ueber phenylhydrazinderivate des α- und β-naphtochinons. Identität des α-derivats mit dem azoderivat des α-naphtols. *Ber. Der Dtsch. Chem. Ges.* **1884**, *17*, 3026–3033. [CrossRef]
18. Antonov, L.; Kurteva, V.; Crochet, A.; Mirolo, L.; Fromm, K.M.; Angelova, S. Tautomerism in 1-phenylazo-4-naphthols: Experimental results vs quantum-chemical predictions. *Dye. Pigment.* **2012**, *92*, 714–723. [CrossRef]
19. Antonov, L.; Hansen, P.E.; van der Zwan, G. Comment on "Spectroscopic studies of keto-enol tautomeric equilibrium of azo dyes" by M. A. Rauf, S. Hisaindee and N. Saleh, RSC Adv. 2015, 5, 18097. *RSC Adv.* **2015**, *5*, 67165–67167. [CrossRef]
20. Hadjoudis, E.; Mavridis, I.M. Photochromism and thermochromism of Schiff bases in the solid state: Structural aspects. *Chem. Soc. Rev.* **2004**. [CrossRef] [PubMed]
21. Raczyńska, E.D.; Kosińska, W.; Ośmiałowski, B.; Gawinecki, R. Tautomeric equilibria in relation to pi-electron delocalization. *Chem. Rev.* **2005**, *105*, 3561–3612. [CrossRef] [PubMed]
22. Kajal, A.; Bala, S.; Kamboj, S.; Sharma, N.; Saini, V. Schiff bases: A versatile pharmacophore. *J. Catal.* **2013**, *2013*, 1–14. [CrossRef]
23. Hansen, P.E. Methods to distinguish tautomeric cases from static ones. In *Tautomerism Concepts and Applications in Science and Technology*; Antonov, L., Ed.; Wiley-VCH: Weinheim, Germany, 2016; pp. 35–74. ISBN 978-3-527-69571-3.
24. Fabian, W.M.F. Quantum chemical calculation of tautomeric equilibria. In *Tautomerism*; Antonov, L., Ed.; Wiley-VCH: Weinheim, Germany, 2013; pp. 337–368. ISBN 978-3-527-65882-4.
25. Antonov, L.; Nedeltcheva, D. Resolution of overlapping UV–Vis absorption bands and quantitative analysis. *Chem. Soc. Rev.* **2000**, *29*, 217–227. [CrossRef]
26. Nedeltcheva, D.; Antonov, L.; Lycka, A.; Damyanova, B.; Popov, S. Chemometric models for quantitative analysis of tautomeric Schiff bases and azo dyes. *Curr. Org. Chem.* **2009**, *13*, 217–240. [CrossRef]
27. Kawauchi, S.; Antonov, L. Description of the tautomerism in some azonaphthols. *J. Phys. Org. Chem.* **2013**, *26*, 643–652. [CrossRef]
28. Neese, F.; Hansen, A.; Wennmohs, F.; Grimme, S. Accurate theoretical chemistry with coupled pair models. *Acc. Chem. Res.* **2009**, *42*, 641–648. [CrossRef] [PubMed]
29. Yang, J.; Waller, M.P. JACOB: A dynamic database for computational chemistry benchmarking. *J. Chem. Inf. Model.* **2012**, *52*, 3255–3262. [CrossRef] [PubMed]
30. Peverati, R.; Truhlar, D.G. Quest for a universal density functional: The accuracy of density functionals across a broad spectrum of databases in chemistry and physics. *Philos. Trans. R. Soc. A Math. Phys. Eng. Sci.* **2014**, *372*, 20120476. [CrossRef] [PubMed]
31. Goerigk, L.; Hansen, A.; Bauer, C.; Ehrlich, S.; Najibi, A.; Grimme, S. A look at the density functional theory zoo with the advanced GMTKN55 database for general main group thermochemistry, kinetics and noncovalent interactions. *Phys. Chem. Chem. Phys.* **2017**, *19*, 32184–32215. [CrossRef] [PubMed]
32. Mehta, N.; Casanova-Páez, M.; Goerigk, L. Semi-empirical or non-empirical double-hybrid density functionals: Which are more robust? *Phys. Chem. Chem. Phys.* **2018**, *20*, 23175–23194. [CrossRef] [PubMed]
33. Morgante, P.; Peverati, R. ACCDB: A Collection of chemistry databases for broad computational purposes. *J. Comput. Chem.* **2019**, *40*, 839–848. [CrossRef]

34. Okawara, M.; Kitao, T.; Hirashima, T.; Matsuoka, M. *Organic Colorants a Handbook of Data of Selected Dyes for Electro-Optical Applications*; Kodansha: Tokyo, Japan; Elsevier: Amsterdam, The Netherlands, 1988; ISBN 978-0-444-98884-3.
35. Savarese, M.; Brémond, É.; Antonov, L.; Ciofini, I.; Adamo, C. Computational insights into excited-state proton-transfer reactions in azo and azomethine dyes. *ChemPhysChem* **2015**, *16*, 3966–3973. [CrossRef]
36. Antonov, L.; Fabian, W.M.F.; Taylor, P.J. Tautomerism in some aromatic Schiff bases and related azo compounds: An LSER study. *J. Phys. Org. Chem.* **2005**, *18*, 1169–1175. [CrossRef]
37. Nedeltcheva, D.; Antonov, L. Relative strength of the intramolecular hydrogen bonding in 1-phenylazo-naphthalen-2-ol and 1-phenyliminomethyl-naphtahlen-2-ol. *J. Phys. Org. Chem.* **2009**, *22*, 274–281. [CrossRef]
38. Stoyanov, S.; Antonov, L. Quantitative analysis of azo-quinonehydrazone tautomeric equilibrium. *Dye. Pigment.* **1989**, *10*, 33–45. [CrossRef]
39. Nedeltcheva, D.; Kurteva, V.; Topalova, I. Gas-phase tautomerism in hydroxy azo dyes—From 4-phenylazo-1-phenol to 4-phenylazo-anthracen-1-ol: Gas-phase tautomerism in hydroxy azo dyes. *Rapid Commun. Mass Spectrom.* **2010**, *24*, 714–720. [CrossRef] [PubMed]
40. Griffiths, J. *Developments in the Chemistry and Technology of Organic Dyes*; Blackwell Scientific Publications: Oxford, UK; Boston, MA, USA, 1984; ISBN 978-0-632-01304-3.
41. Fabian, W.M.F.; Antonov, L.; Nedeltcheva, D.; Kamounah, F.S.; Taylor, P.J. Tautomerism in hydroxynaphthaldehyde anils and azo analogues: A combined experimental and computational study. *J. Phys. Chem. A* **2004**, *108*, 7603–7612. [CrossRef]
42. Peverati, R.; Truhlar, D.G. Screened-exchange density functionals with broad accuracy for chemistry and solid-state physics. *Phys. Chem. Chem. Phys.* **2012**, *14*, 16187. [CrossRef] [PubMed]
43. Becke, A.D. A new mixing of Hartree–Fock and local density-functional theories. *J. Chem. Phys.* **1993**, *98*, 1372–1377. [CrossRef]
44. Zhao, Y.; Truhlar, D.G. The M06 suite of density functionals for main group thermochemistry, thermochemical kinetics, noncovalent interactions, excited states, and transition elements: Two new functionals and systematic testing of four M06-class functionals and 12 other functionals. *Theor. Chem. Acc.* **2008**, *120*, 215–241.
45. Roothaan, C.C.J. New developments in molecular orbital theory. *Rev. Mod. Phys.* **1951**, *23*, 69–89. [CrossRef]
46. Peverati, R.; Truhlar, D.G. Communication: A global hybrid generalized gradient approximation to the exchange-correlation functional that satisfies the second-order density-gradient constraint and has broad applicability in chemistry. *J. Chem. Phys.* **2011**, *135*, 191102. [CrossRef]
47. Peverati, R.; Truhlar, D.G. Improving the accuracy of hybrid meta-gga density functionals by range separation. *J. Phys. Chem. Lett.* **2011**, *2*, 2810–2817. [CrossRef]
48. Yanai, T.; Tew, D.P.; Handy, N.C. A new hybrid exchange–correlation functional using the Coulomb-attenuating method (CAM-B3LYP). *Chem. Phys. Lett.* **2004**, *393*, 51–57. [CrossRef]
49. Henderson, T.M.; Izmaylov, A.F.; Scuseria, G.E.; Savin, A. Assessment of a middle-range hybrid functional. *J. Chem. Theory Comput.* **2008**, *4*, 1254–1262. [CrossRef] [PubMed]
50. Chai, J.-D.; Head-Gordon, M. Systematic optimization of long-range corrected hybrid density functionals. *J. Chem. Phys.* **2008**, *128*, 084106. [CrossRef] [PubMed]
51. Adamo, C.; Barone, V. Toward reliable density functional methods without adjustable parameters: The PBE0 model. *J. Chem. Phys.* **1999**, *110*, 6158–6170. [CrossRef]
52. Ernzerhof, M.; Perdew, J.P. Generalized gradient approximation to the angle- and system-averaged exchange hole. *J. Chem. Phys.* **1998**, *109*, 3313–3320. [CrossRef]
53. Austin, A.; Petersson, G.A.; Frisch, M.J.; Dobek, F.J.; Scalmani, G.; Throssell, K. A density functional with spherical atom dispersion terms. *J. Chem. Theory Comput.* **2012**, *8*, 4989–5007. [CrossRef] [PubMed]
54. Chai, J.-D.; Head-Gordon, M. Long-range corrected hybrid density functionals with damped atom—Atom dispersion corrections. *Phys. Chem. Chem. Phys.* **2008**, *10*, 6615. [CrossRef] [PubMed]
55. Krukau, A.V.; Vydrov, O.A.; Izmaylov, A.F.; Scuseria, G.E. Influence of the exchange screening parameter on the performance of screened hybrid functionals. *J. Chem. Phys.* **2006**, *125*, 224106. [CrossRef]
56. Vydrov, O.A.; Scuseria, G.E. Assessment of a long-range corrected hybrid functional. *J. Chem. Phys.* **2006**, *125*, 234109. [CrossRef]
57. Becke, A.D. Density-functional exchange-energy approximation with correct asymptotic behavior. *Phys. Rev. A* **1988**, *38*, 3098–3100. [CrossRef]

58. Becke, A.D. Density-functional thermochemistry. III. The role of exact exchange. *J. Chem. Phys.* **1993**, *98*, 5648–5652. [CrossRef]
59. Xu, X.; Goddard, W.A. From the cover: The X3LYP extended density functional for accurate descriptions of nonbond interactions, spin states, and thermochemical properties. *Proc. Natl. Acad. Sci. USA* **2004**, *101*, 2673–2677. [CrossRef] [PubMed]
60. Møller, C.; Plesset, M.S. Note on an approximation treatment for many-electron systems. *Phys. Rev.* **1934**, *46*, 618–622. [CrossRef]
61. Becke, A.D. Density functional calculations of molecular bond energies. *J. Chem. Phys.* **1986**, *84*, 4524–4529. [CrossRef]
62. Lee, C.; Yang, W.; Parr, R.G. Development of the Colle-Salvetti correlation-energy formula into a functional of the electron density. *Phys. Rev. B* **1988**, *37*, 785–789. [CrossRef]
63. Staroverov, V.N.; Scuseria, G.E.; Tao, J.; Perdew, J.P. Comparative assessment of a new nonempirical density functional: Molecules and hydrogen-bonded complexes. *J. Chem. Phys.* **2003**, *119*, 12129–12137. [CrossRef]
64. Boese, A.D.; Handy, N.C. New exchange-correlation density functionals: The role of the kinetic-energy density. *J. Chem. Phys.* **2002**, *116*, 9559–9569. [CrossRef]
65. Tao, J.; Perdew, J.P.; Staroverov, V.N.; Scuseria, G.E. Climbing the density functional ladder: Nonempirical meta–generalized gradient approximation designed for molecules and solids. *Phys. Rev. Lett.* **2003**, 91. [CrossRef]
66. Handy, N.C.; Cohen, A.J. Left-right correlation energy. *Mol. Phys.* **2001**, *99*, 403–412. [CrossRef]
67. Cohen, A.J.; Handy, N.C. Dynamic correlation. *Mol. Phys.* **2001**, *99*, 607–615. [CrossRef]
68. Boese, A.D.; Martin, J.M.L. Development of density functionals for thermochemical kinetics. *J. Chem. Phys.* **2004**, *121*, 3405–3416. [CrossRef]
69. Crochet, A.; Fromm, K.M.; Kurteva, V.; Antonov, L. (E)-1-(4-Methoxyanthracen-1-yl)-2-phenyldiazene. *Acta Crystallogr. Sect. E Struct. Rep. Online* **2011**, *67*, o993. [CrossRef] [PubMed]
70. Gilli, P.; Bertolasi, V.; Pretto, L.; Antonov, L.; Gilli, G. Variable-temperature X-ray crystallographic and DFT computational study of the N-H···O/N···H-O tautomeric competition in 1-(Arylazo)-2-naphthols. Outline of a transiton-state hydrogen-bond theory. *J. Am. Chem. Soc.* **2005**, *127*, 4943–4953. [CrossRef] [PubMed]
71. Nedeltcheva, D.; Kamounah, F.S.; Mirolo, L.; Fromm, K.M.; Antonov, L. Solid state tautomerism in 2-((phenylimino)methyl)naphthalene-1-ol. *Dye. Pigment.* **2009**, *83*, 121–126. [CrossRef]
72. Antonov, L. Absorption UV-Vis Spectroscopy and chemometrics: from qualitative conclusions to quantitative analysis. In *Tautomerism: Methods and Theories*; Antonov, L., Ed.; Wiley-VCH: Weinheim, Germany, 2013; pp. 25–47. ISBN 978-3-527-65882-4.
73. Antonov, L.; Fabian, W.M.F.; Nedeltcheva, D.; Kamounah, F.S. Tautomerism of 2-hydroxynaphthaldehyde Schiff bases. *J. Chem. Soc. Perkin Trans. 2* **2000**, 1173–1179. [CrossRef]
74. Ali, S.T.; Antonov, L.; Fabian, W.M.F. Phenol–quinone tautomerism in (Arylazo)naphthols and the analogous Schiff bases: Benchmark calculations. *J. Phys. Chem. A* **2014**, *118*, 778–789. [CrossRef] [PubMed]
75. Frisch, M.J.; Trucks, G.W.; Schlegel, H.B.; Scuseria, G.E.; Robb, M.A.; Cheeseman, J.R.; Scalmani, G.; Barone, V.; Mennucci, B.; Petersson, G.A.; et al. *Gaussian 09 Revision D.01*; Gaussian Inc.: Wallingford, CT, USA, 2013.
76. Tomasi, J.; Mennucci, B.; Cammi, R. Quantum mechanical continuum solvation models. *Chem. Rev.* **2005**, *105*, 2999–3094. [CrossRef] [PubMed]
77. Scuseria, G.E.; Schaefer, H.F. Is coupled cluster singles and doubles (CCSD) more computationally intensive than quadratic configuration interaction (QCISD)? *J. Chem. Phys.* **1989**, *90*, 3700–3703. [CrossRef]
78. Miehlich, B.; Savin, A.; Stoll, H.; Preuss, H. Results obtained with the correlation energy density functionals of becke and Lee, Yang and Parr. *Chem. Phys. Lett.* **1989**, *157*, 200–206. [CrossRef]
79. Vosko, S.H.; Wilk, L.; Nusair, M. Accurate spin-dependent electron liquid correlation energies for local spin density calculations: A critical analysis. *Can. J. Phys.* **1980**, *58*, 1200–1211. [CrossRef]
80. Nelder, J.A.; Mead, R. A Simplex method for function minimization. *Comput. J.* **1965**, *7*, 308–313. [CrossRef]

Sample Availability: Samples of the compounds are not available from the author.